Title	Davydov Ansatz as an efficient tool for the simulation of nonlinear optical response of molecular aggregates
Author(s)	Sun, Ke-Wei; Gelin, Maxim F.; Chernyak, Vladimir Y.; Zhao, Yang
Citation	Sun, K.-W., Gelin, M. F., Chernyak, V. Y., & Zhao, Y. (2015). Davydov Ansatz as an efficient tool for the simulation of nonlinear optical response of molecular aggregates. Journal of chemical physics, 142, 212448-.
Date	2015
URL	http://hdl.handle.net/10220/25928
Rights	© 2015 American Institute of Physics. This is the author created version of a work that has been peer reviewed and accepted for publication by Journal of Chemical Physics, American Institute of Physics. It incorporates referee's comments but changes resulting from the publishing process, such as copyediting, structural formatting, may not be reflected in this document. The published version is available at: [http://dx.doi.org/10.1063/1.4921575].

Davydov ansatz as an efficient tool for the simulation of nonlinear optical response of molecular aggregates

Ke-Wei Sun[1,2], Maxim F. Gelin[3], Vladimir Y. Chernyak[2,4], and Yang Zhao[2*]
[1] *School of Science, Hangzhou Dianzi University, Hangzhou 310018, China*
[2] *Division of Materials Science, Nanyang Technological University, 50 Nanyang Avenue, Singapore 639798*
[3] *Department of Chemistry, Technische Universität München, Garching, D-85747, Germany*
[4] *Department of Chemistry, Wayne State University, Detroit, USA*
(Dated: May 12, 2015)

We have developed a variational approach to the description of four-wave-mixing signals of molecular aggregates, in which the third-order response functions are evaluated in terms of the Davydov ansätze. Our theory treats both singly- and doubly-excited excitonic states, handling the contributions due to stimulated emission, ground state bleach, and excited state absorption. As an illustration, we simulate a series of optical two-dimensional (2D) spectra of model J-aggregates. Our approach may become suitable for the computation of femtosecond optical four-wave-mixing signals of molecular aggregates with intermediate-to-strong exciton-phonon and exciton-exciton couplings.

PACS numbers:

I. INTRODUCTION

Nonlinear optical spectroscopy comprises a family of techniques such as fluorescence up-conversion, pump-probe, transient grating, photon echo, coherent anti-Stokes-Raman scattering, etc., which generally are referred to as four-wave-mixing spectroscopies [1]. These techniques differ in the number, ordering, and phase-matching directions of the pulses involved and in the specific informations they deliver on the material system under study. However, all these techniques share one fundamental property: The corresponding signals are uniquely determined by the third-order polarization $P(t)$.

The perturbative evaluation of the nonlinear polarization expresses $P(t)$ as a triple time integral involving the nonlinear response function [1]

$$P(t) = \int_0^\infty dt_1 \int_0^\infty dt_2 \int_0^\infty dt_3 \; S(t_1,t_2,t_3)E(t-t_3) \times E(t-t_3-t_2)E(t-t_3-t_2-t_1). \quad (1)$$

Here $E(t)$ represents the electric field of the pulses involved and depends parametrically on their carrier frequencies, phases, and mutual delays. The response function $S(t_1,t_2,t_3)$ represents the system dynamics in the absence of external fields. For simple material systems, such as few-level systems or damped harmonic oscillators, $S(t_1,t_2,t_3)$ can be calculated analytically [1]. The evaluation of the response functions for molecular aggregates necessitates, usually, additional simplifying assumptions, resulting in the perturbative treatment of off-diagonal excitonic fluctuations [2, 3], system-bath couplings [4, 5], or other approximations [6–11].

The approaches of Refs. [2–8] are popular methods of choice in practical simulations of spectroscopic signals. Yet molecular aggregates are characterized by moderate to strong exciton-exciton and exciton-phonon coupling strengths [4, 12, 13]. An adequate simulation of the dynamics of such complexes necessitates a non-perturbative treatment of these couplings. The corresponding computational methods are available: The Hierarchy Equation of Motion approach (HEOM) [14–16], the multiconfigurational time-dependent Hartree (MCTDH) method [17–19], hierarchical approximations of the bath spectral density [20, 21], the numerical renormalization group approach [22, 23], and the quasiadiabatic propagator path integral (QUAPI) [24, 25]. If the system-bath Hamiltonian possesses a certain symmetry, it is possible to derive exact quantum master equations [26, 27].

Recent years have witnessed considerable progress in the studies of dynamics of quantum dissipative systems by numerically exact methods. For example, benchmark calculations of the 7-site (QUAPI, [28]) and 24-site (HEOM, [29]) Fenna-Matthews-Olson (FMO) complex have been performed, two-dimensional (2D) electronic spectra of FMO have been simulated (HEOM, [30–32]), 2D spectra of a two-vibrational-mode electron-transfer system have been calculated (HEOM, [33]), and various femtosecond signals for polyatomic molecules with multiple vibrational modes have been computed (MCTDH, [19]).

Yet the application of the exact methods of Refs. [14–25] to the simulation of the dynamics of molecular aggregates with multiple exciton-exciton and exciton-phonon couplings is beyond the capacity of the present-day computers. The application of these methods for the computation of third-order spectroscopic signals, either in terms of nonlinear response functions or by using the schemes treating the system-field interactions non-perturbatively [34–36], is even more computationally demanding.

In the present work, we use a computationally efficient approach capable of tackling such systems. It is based on the Frenkel-Dirac variational time-dependent method for the construction of the Davydov ansätze [37–45]. Re-

*Electronic address: YZhao@ntu.edu.sg

cently, this approach has been adopted to simulate inter- and intra-ring dynamics in various arrays of molecular rings and yielded accurate results for the energy transfer dynamics over a wide range of the exciton-phonon coupling strengths [46–48].

Our aim is the evaluation of the third order response functions of molecular aggregates in terms of the Davydov ansätze. This project was initiated by our work [49], in which we restricted our consideration to the singly-excited excitonic states. Here, we extend the description towards doubly-excited excitonic states, which are necessary for a proper accounting for excited-state absorption. This is the most significant result of the present work (see Section IV), which permits the development of a general theory of four-wave-mixing spectroscopy of excitonic systems.

The rest of the paper is organized as follows. Section II defines relevant Hamiltonians. Sections III and IV contain detailed derivations and explicit working formulas for the response functions. Section V recapitulates and systematizes the findings of Sections III and IV. In Section VI, we employ the D_1 ansatz for the simulation of optical 2D spectra of a model J-aggregate. Our main results are briefly summarized in Section VII.

II. HAMILTONIAN

We consider one-dimensional molecular ring comprised of N interacting chromophores (for example, BChls-a) embedded in a protein environment. The total Hamiltonian for this model can be partitioned into the system Hamiltonian, the bath Hamiltonian, and their coupling,

$$H = H_S + H_B + H_{SB}. \tag{2}$$

Following the discussion in Refs. [49, 50], we incorporate high-frequency vibrational modes with significant exciton-phonon coupling into the system Hamiltonian and treat them explicitly. All other vibrational modes are assumed to form a heat bath.

The system is specified by a Holstein Hamiltonian describing excitations in the molecular ring [51]:

$$H_S = H_{\rm ex} + H_{\rm ph} + H_{\rm ex-ph}. \tag{3}$$

$H_{\rm ex}$ is the Frenkel-exciton Hamiltonian

$$H_{\rm ex} = \sum_{m=1}^{N} \varepsilon_m B_m^\dagger B_m + \sum_{m=1}^{N}\sum_{n\neq m} J_{mn} B_m^\dagger B_n + \frac{1}{2}\sum_{m=1}^{N}\sum_{n\neq m} K_{mn} B_m^\dagger B_n^\dagger B_m B_n. \tag{4}$$

Here $B_m^\dagger$ (B_m) creates (annihilates) excitation at the site m, J_{nm} is the resonant coupling between the excitons n and m, while K_{mn} is the so-called quadratic coupling [7, 8].

$H_{\rm ph}$ is the phonon Hamiltonian which describes the primary vibrations of the molecular ring ($\hbar = 1$)

$$H_{\rm ph} = \sum_q \omega_q b_q^\dagger b_q, \tag{5}$$

and $H_{\rm ex-ph}$ is responsible for the exciton-phonon coupling which is assumed to be site-diagonal

$$H_{\rm ex-ph} = \sum_q \sum_{m=1}^{N} g_q \omega_q \left(b_q e^{-iqm} + b_q^\dagger e^{iqm} \right) B_m^\dagger B_m. \tag{6}$$

b_q ($b_q^\dagger$) denotes the annihilation (creation) operator of the primary phonon with frequency ω_q, g_q is the exciton-phonon coupling strength, and dimensionless momentum $q = 2\pi n_q/N$ ($n_q = -7, -6, ..., 8$), where $N = 16$. We assume a linear dispersion for the primary phonon,

$$\omega_q = \omega_0 + 2W\left(|q|/\pi - 1/2\right), \tag{7}$$

and consider the elliptic form of the phonon bath correlation function

$$\begin{aligned} C_{00}(\omega) &= \frac{1}{N}\sum_q g_q^2 \omega_q^2 \delta(\omega - \omega_q) \\ &= \frac{2S\omega^2}{N\pi W^2}\sqrt{W^2 - (\omega - \omega_0)^2}. \end{aligned} \tag{8}$$

Here ω_0 is the central phonon frequency and W is the frequency bandwidth.

The exciton-phonon coupling can conveniently be characterized via the Huang-Rhys factor S defined by the relation

$$\frac{1}{N}\sum_q g_q^2 \omega_q = S\omega_0. \tag{9}$$

Here g_q can be obtained from Eqs. (7)-(9) for given Huang-Rhys factor S and phonon bandwidth W [43].

The second and the third terms in Eq. (2) describe interaction of the system with low-frequency intramolecular vibrations of BChls-a and with nuclear degrees of freedom of the environment. Having incorporated the vibrational modes with strong exciton-phonon coupling into H_S, we may utilize a rather simplified description of H_B and H_{SB}. Motivated by the symmetry of the molecular ring, we assume a harmonic bath with site-independent diagonal couplings to the system excitonic states:

$$H_B = \sum_j \Omega_j a_j^\dagger a_j, \tag{10}$$

$$H_{SB} = \hat{N} h_{SB}. \tag{11}$$

Here a_j ($a_j^\dagger$) is the annihilation (creation) operator of a phonon of the bath with frequency Ω_j,

$$\hat{N} = \sum_{m=1}^{N} B_m^\dagger B_m \tag{12}$$

is the excitonic number operator, and

$$h_{SB} = \sum_j \kappa_j \hbar \Omega_j \left(a_j + a_j^\dagger \right), \tag{13}$$

κ_j being the coupling strength of the exciton to the jth bath mode. The bath spectral density is defined as

$$D(\omega) = \sum_j \kappa_j^2 \Omega_j^2 \delta(\omega - \Omega_j). \tag{14}$$

We thus consider a simple form of exciton-phonon interactions in which the collective coordinate of the bath is coupled to the number of excitons operator. For such coupling the bath Hamiltonian, with the coupling term included, commutes with the exciton number, and as a result, the nonlinear response can be factorized into the response of the system (excitons coupled to high-frequency phonons) and the response of a three-level system, diagonally coupled to a harmonic bath (see Section III); the latter response, as well known [1], can be computed exactly within the multi-mode Brownian oscillator model. The reason of our selection of coupling is that the intent here is to focus on the effects of exciton interactions with high-frequency phonons, and how to treat the latter within the framework of time-dependent variation. The bath was added to obtain smooth signals, and therefore, the one that can be handled in the easiest way was our primary choice.

III. THIRD-ORDER RESPONSE FUNCTIONS

A. Starting equations

Let

$$\hat{\mu} = \sum_{m=1}^{N} c_m (B_m^\dagger + B_m) \equiv \hat{\mu}_+ + \hat{\mu}_- \tag{15}$$

be the total transition dipole moment operator. Here

$$c_m = (\boldsymbol{e}\boldsymbol{\mu}_m), \tag{16}$$

$\boldsymbol{\mu}_m$ are the unit vectors ($|\boldsymbol{\mu}_m| = 1$) of the transition dipoles, and $\boldsymbol{e}$ is the unit vector specifying linear polarization of the laser pulses. For convenience, we assume that all laser pulses have the same polarization and incorporate it into the definition of $\hat{\mu}$.

The fundamental quantity describing the third-order response of the system on the external fields is the four-time correlation function of the transition dipole moment operators [1],

$$\Phi(\tau_4, \tau_3, \tau_2, \tau_1) = \langle \hat{\mu}(\tau_4)\hat{\mu}(\tau_3)\hat{\mu}(\tau_2)\hat{\mu}(\tau_1) \rangle . \tag{17}$$

Here the actual times τ_1, τ_2, τ_3, and τ_4 are not necessarily chronologically ordered and the Heisenberg operators

$$\hat{\mu}(\tau) = e^{iH\tau} \hat{\mu} e^{-iH\tau} \tag{18}$$

are governed by the total Hamiltonian H. The angular brackets in Eq. (17) mean the trace over vibrational and excitonic degrees of freedom. Since the high-frequency vibrational modes are incorporated into the system Hamiltonian H_S, we assume that the system before the interaction with the laser pulses resides in its ground excitonic state and its ground vibrational state $|\Psi_0\rangle$. Hence

$$\langle ... \rangle \equiv \mathrm{Tr}_B \{ \rho_B \langle \Psi_0 | ... | \Psi_0 \rangle \} \tag{19}$$

where

$$\rho_B = Z_B^{-1} \exp\{-\beta H_B\} \tag{20}$$

is the equilibrium distribution over the bath phonons at a temperature T_{eq}. Here Z_B is the partition function, $\beta = (k_B T_{eq})^{-1}$, and k_B is the Boltzmann constant.

Within the wave function formalism [1], there are four contributions to the third-order response function of Eq. (1):

$$S(t_1, t_2, t_3) = -i \sum_{k=1}^{4} \{ R_k(t_3, t_2, t_1) - [R_k(t_3, t_2, t_1)]^* \}. \tag{21}$$

All the four contributions can be expressed in terms of the four-time correlation function (17) as follows [1]:

$$R_1(t_3, t_2, t_1) = \Phi(t_1, t_1 + t_2, t_1 + t_2 + t_3, 0), \tag{22}$$

$$R_2(t_3, t_2, t_1) = \Phi(0, t_1 + t_2, t_1 + t_2 + t_3, t_1), \tag{23}$$

$$R_3(t_3, t_2, t_1) = \Phi(0, t_1, t_1 + t_2 + t_3, t_1 + t_2), \tag{24}$$

$$R_4(t_3, t_2, t_1) = \Phi(t_1 + t_2 + t_3, t_1 + t_2, t_1, 0), \tag{25}$$

According to Refs. [2, 3], the auxiliary correlation function Φ can be expressed as a sum of two contributions Φ^{s} and Φ^{d}, which correspond to the two situations in which, during the evolution from τ_2 to τ_3, the system is electronically in the ground and the two-exciton excited states, respectively (in both cases from τ_1 to τ_2 and from τ_3 to τ_4 the system is in one-exciton state):

$$\Phi(\tau_4, \tau_3, \tau_2, \tau_1) = \Phi^s(\tau_4, \tau_3, \tau_2, \tau_1) + \Phi^d(\tau_4, \tau_3, \tau_2, \tau_1). \tag{26}$$

Explicitly,

$$\Phi^s(\tau_4, \tau_3, \tau_2, \tau_1) = \langle \hat{\mu}_-(\tau_4)\hat{\mu}_+(\tau_3)\hat{\mu}_-(\tau_2)\hat{\mu}_+(\tau_1) \rangle \tag{27}$$

and

$$\Phi^d(\tau_4, \tau_3, \tau_2, \tau_1) = \langle \hat{\mu}_-(\tau_4)\hat{\mu}_-(\tau_3)\hat{\mu}_+(\tau_2)\hat{\mu}_+(\tau_1) \rangle . \tag{28}$$

B. Separation of the system and bath contributions

The system Hamiltonian H_S commutes with the bath Hamiltonian H_B and the system-bath coupling H_{SB}. Hence,

$$\hat{\mu}_-(\tau) = e^{iH_S\tau} e_-^{i\int_0^\tau d\tau' H_{SB}(\tau')} \hat{\mu}_- e_+^{-i\int_0^\tau d\tau' H_{SB}(\tau')} e^{-iH_S\tau} \tag{29}$$

where

$$H_{SB}(\tau) = e^{iH_B\tau} H_{SB} e^{-iH_B\tau} \tag{30}$$

Furthermore, the excitonic operators enter $H_{SB}(\tau) \equiv \hat{N} h_{SB}(\tau)$ only through the number operator $\hat{N}$ defined per Eq. (12). Therefore

$$\hat{\mu}_-(\tau) = e^{iH_S\tau} \hat{\mu}_- e^{-iH_S\tau} U(\tau) \tag{31}$$

where

$$U(\tau) \equiv e_+^{-i\int_0^\tau d\tau' h_{SB}(\tau')}. \tag{32}$$

Hence the dynamics governed by $H_{SB} + H_B$ and H_S can be separated, and the four-time response function can be represented as a product of the bath (F^α) and system (G^α) counterparts:

$$\Phi^\alpha(\tau_4, \tau_3, \tau_2, \tau_1) = F^\alpha(\tau_4, \tau_3, \tau_2, \tau_1) G^\alpha(\tau_4, \tau_3, \tau_2, \tau_1) \tag{33}$$

($\alpha = s, d$).

A common procedure for the construction of the nonlinear response functions is as follows [2, 3, 7, 8]. One diagonalizes the exciton Hamiltonian $H_{\rm ex}$, evaluates diagonal fluctuations exactly, and treats off-diagonal fluctuations at different levels of approximation. In the present case, due to the symmetry of H_B and H_{SB}, we do not need to diagonalize $H_{\rm ex}$ and resort to additional approximations. The bath is responsible for electronic dephasing, which must be taken into account for an adequate description of nonlinear optical responses.

C. Bath response functions

According to Eq. (31), the single- and double-exciton four-time bath response functions are defined as follows:

$$F^s(\tau_4, \tau_3, \tau_2, \tau_1) = {\rm Tr}_B\{\rho_B U(\tau_4) U^\dagger(\tau_3) U(\tau_2) U^\dagger(\tau_1)\}, \tag{34}$$

$$F^d(\tau_4, \tau_3, \tau_2, \tau_1) = {\rm Tr}_B\{\rho_B U(\tau_4) U(\tau_3) U^\dagger(\tau_2) U^\dagger(\tau_1)\}. \tag{35}$$

By using the cumulant expansion, the above correlation functions are evaluated exactly [2]:

$$F^s(\tau_4, \tau_3, \tau_2, \tau_1) = \exp\{-[g(\tau_2 - \tau_1) - g(\tau_3 - \tau_1)$$

$$+g(\tau_4 - \tau_1) + g(\tau_3 - \tau_2) - g(\tau_4 - \tau_2) + g(\tau_4 - \tau_3)]\}, \tag{36}$$

$$F^d(\tau_4, \tau_3, \tau_2, \tau_1) = \exp\{-[-g(\tau_2 - \tau_1) + g(\tau_3 - \tau_1)$$

$$+g(\tau_4 - \tau_1) + g(\tau_3 - \tau_2) + g(\tau_4 - \tau_2) - g(\tau_4 - \tau_3)]\}. \tag{37}$$

Here, the lineshape functions are expressed through the bath spectral density (14):

$$g(t) = \int_0^\infty d\omega \frac{D(\omega)}{\omega^2} [\coth\frac{\beta\hbar\omega}{2}(1 - \cos\omega t) + i(\sin\omega t - \omega t)]. \tag{38}$$

IV. SYSTEM RESPONSE FUNCTIONS IN TERMS OF DAVYDOV ANSÄTZE

The single-exciton and double-exciton four-time system response functions read:

$$G^s(\tau_4, \tau_3, \tau_2, \tau_1) = \langle\Psi_0|\hat{\mu}_- e^{-iH_S(\tau_4 - \tau_3)} \hat{\mu}_+ \times e^{-iH_{\rm ph}(\tau_3 - \tau_2)} \hat{\mu}_- e^{-iH_S(\tau_2 - \tau_1)} \hat{\mu}_+ |\Psi_0\rangle, \tag{39}$$

$$G^d(\tau_4, \tau_3, \tau_2, \tau_1) = \langle\Psi_0|\hat{\mu}_- e^{-iH_S(\tau_4 - \tau_3)} \hat{\mu}_- \times e^{-iH_S(\tau_3 - \tau_2)} \hat{\mu}_+ e^{-iH_S(\tau_2 - \tau_1)} \hat{\mu}_+ |\Psi_0\rangle. \tag{40}$$

In writing the above expressions, we have made use of the fact that (i) H_S conserves the number of excitons and (ii) the energy of the ground exciton-vibrational state is set to zero,

$$H_S|\Psi_0\rangle = 0. \tag{41}$$

In addition, $\exp\{-iH_S(\tau_3 - \tau_2)\}$ is replaced by $\exp\{-iH_{\rm ph}(\tau_3 - \tau_2)\}$ in the single-exciton response function, since the system is its ground excitonic state during $\tau_3 - \tau_2$.

Below we show how to evaluate the single-exciton response function (39) and the double-exciton response function (40) in terms of the Davydov D_1 ansätze. This is the most significant part of the present work, which is based on several technical considerations. Below we consider G^s and G^d separately.

A. Single-exciton response function

To set up the stage, we begin with the qualitative discussion of the linear response. In this case application of the D_1 ansatz is straightforward due to the following reasons. At room temperatures both the excitonic and the high-frequency phonon components are in their ground states labeled by $|\Psi_0\rangle$, which obviously belongs to the class of the D_1 trial states. It is easy to see that application of the dipole operator $\hat{\mu}$ of Eq. (15) on the system ground state, which represents interactions with the driving field, results in $|\hat{\mu}\Psi_0\rangle$ with its D_1 nature preserved. Therefore the system dynamics during the only time interval involved in the description of the time-domain linear response can be approximately treated using the dynamical version of the D_1 ansatz, leading to the state

$$|\mathcal{U}(\hat{\mu}\Psi_0; t)\rangle \equiv \sum_j^N A_j(t) \exp\Big\{\sum_q \big[\lambda_{j,q}(t)\hat{b}_q^\dagger - {\rm H.c.}\big]\Big\} \otimes |j\rangle. \tag{42}$$

Here

$$|j\rangle \equiv B_j^\dagger|\Psi_0\rangle \tag{43}$$

and the parameters of the ansatz obey the initial conditions

$$A_j(0) = c_j, \quad \lambda_{j,q}(0) = 0. \tag{44}$$

The equations of motion for the dynamic parameters $A_j(t)$ and $\lambda_{j,q}(t)$ are derived from the Dirac-Frenkel variational principle as explained in the Appendix. Note that the propagation operator for the dynamical D_1 ansatz, $\mathcal{U}(t)$, is a nonlinear one that acts in the space of the D_1 trial states, the latter not being a vector space. The final step of computation of the matrix element of the dipole operator between the evolving D_1 state and the ground state boils down to a straightforward evaluation of $\langle\Psi_0|\hat{\mu}\mathcal{U}(\hat{\mu}\Psi_0;t)\rangle$. Such linear response functions have been used for the interpretation of femtosecond single-molecule experiments on light-harvesting complexes [52].

Application of the D_1 ansatz to the third order response is apparently much less straightforward. Consider the $G^{\rm s}$ contribution first. Propagation from τ_1 to τ_2 occurs in the one-exciton state and can be treated in the same fashion as the case of linear response using the D_1 ansatz approach, resulting in $|\mathcal{U}(\hat{\mu}\Psi_0;\tau_2-\tau_1)\rangle$. Application of the annihilation component of the dipole operator produces a linear superposition $\sum_{j=1}^{N} c_j|\mathcal{P}_j\mathcal{U}(\hat{\mu}\Psi_0;\tau_2-\tau_1)\rangle$ of coherent phonon states $|\mathcal{P}_j\mathcal{U}(\hat{\mu}\Psi_0;\tau_2-\tau_1)\rangle$, with $\mathcal{P}_j$ denoting the projection operator onto the jth chromophore. In the zero-exciton sector, our Hamiltonian preserves the coherent state (or equivalently, the D_1 ansatz in the zero-exciton sector is exact), so that propagation from τ_2 to τ_3 results in $\sum_{j=1}^{N} c_j|\mathcal{U}(\mathcal{P}_j\mathcal{U}(\hat{\mu}\Psi_0;\tau_2-\tau_1);\tau_3-\tau_2)\rangle$, i.e., in a superposition of N coherent states. Acting with a dipole operator will produce a superposition of N D_1 states; each of those can be propagated from τ_3 to τ_4 using the D_1 ansatz. However, to reduce the numerical effort by the factor of N we use the following (obvious) trick: instead of propagating N D_1 states, as described above, we act with the dipole operator on the bra ground state $\langle\Psi_0|$, propagate it "backward" [54] in time from τ_4 to τ_1 and further act with the annihilation component of the dipole operator resulting in $\sum_{k=1}^{N} c_k^*\langle(\mathcal{P}_k\mathcal{U}(\hat{\mu}\Psi_0;\tau_3-\tau_4))|$. The contribution $G^{\rm s}$ is finally obtained in a straightforward way by summing up N^2 scalar products of coherent state:

$$G^{\rm s}(\tau_4,\tau_3,\tau_2,\tau_1) = \sum_{jk}^{N} c_j c_k^* \langle\mathcal{P}_k\mathcal{U}(\hat{\mu}\Psi_0;\tau_3-\tau_4)| \times |\mathcal{U}(\mathcal{P}_j\mathcal{U}(\hat{\mu}\Psi_0;\tau_2-\tau_1);\tau_3-\tau_2)\rangle. \tag{45}$$

The explicit evaluation of this expression in terms of the Davydov ansatz (42) yields the following working formula for the single-exciton response function [49, 53]:

$$G^{s}(\tau_4,\tau_3,\tau_2,\tau_1) = \sum_{jk}^{N} c_j c_k^* [A_k(\tau_3-\tau_4)]^* A_j(\tau_2-\tau_1) \times e^{-\frac{1}{2}\sum_q\left(|\lambda_{k,q}(\tau_3-\tau_4)|^2+|\lambda_{j,q}(\tau_2-\tau_1)|^2\right)} \times e^{\sum_q\left(e^{-i\omega_q(\tau_3-\tau_2)}[\lambda_{k,q}(\tau_3-\tau_4)]^*\lambda_{j,q}(\tau_2-\tau_1)\right)}. \tag{46}$$

B. Double-exciton response function

The contribution $G^{\rm d}$ that involves the two-exciton states in the τ_2 to τ_3 evolution is computed in a similar fashion by first propagating $|\hat{\mu}\Psi_0\rangle$ and $\langle\hat{\mu}\Psi_0|$ from τ_1 to τ_2 and from τ_4 from τ_3, respectively. Propagation between τ_2 and τ_3 occurs, however, in the two-exciton state sector, since we act on the state $|\mathcal{U}(\hat{\mu}\Psi_0;\tau_2-\tau_1)\rangle$ with the creation component of the dipole operator. This results in a two-exciton state

$$\sum_{jk}^{k\neq j} c_j|\mathcal{P}_k\mathcal{U}(\hat{\mu}\Psi_0;\tau_2-\tau_1)\rangle\otimes|jk\rangle, \tag{47}$$

$$|jk\rangle \equiv B_j^\dagger B_k^\dagger|\Psi_0\rangle. \tag{48}$$

Conceptually, the double-exciton D_1 ansatz is a straightforward extension of the single-exciton D_1 counterpart, where a trial state is represented by a superposition $\sum_{jk}^{j<k}|\Psi_{jk}\rangle\otimes|jk\rangle$, with $|\Psi_{jk}\rangle$ being represented by the coherent states of the vibrational variables (see, e.g., Refs. [55, 56]). The state defined by Eq. (47) is not, as might seem to be at the first sight, a D_1-type state, since in the electronic space $|jk\rangle = |kj\rangle$, so that each two-exciton state in the site representation is weighted with a linear superposition of two sets of coherent states, rather than a single one, the latter being the requirement of the D_1 ansatz. However, Eq. (47) is obviously represented by a linear superposition of the $N(N-1)$ two-exciton D_1 states, so that each of the latter can be propagated using the D_1 ansatz, resulting in a superposition of $N(N-1)$ D_1 states [57]. Applying the similar arguments we have used earlier to obtain the $G^{\rm s}$ contribution, we arrive at

$$G^{\rm d}(\tau_4,\tau_3,\tau_2,\tau_1) = \sum_{ijkl}^{N} c_i c_k^* \langle kl|\otimes\langle\mathcal{P}_l\mathcal{U}(\hat{\mu}\Psi_0;\tau_3-\tau_4)|\times |\mathcal{U}(\mathcal{P}_j\mathcal{U}(\hat{\mu}\Psi_0;\tau_2-\tau_1)\otimes|ij\rangle;\tau_3-\tau_2)\rangle. \tag{49}$$

This expression can explicitly be evaluated in terms of the Davydov ansätze as follows. $\langle\mathcal{U}(\hat{\mu}\Psi_0;\tau_3-\tau_4)|$ is nothing else than the single-exciton Davydov ansatz propagated "backward" in time, which was introduced in Section IV A. As for the ket part, it can be expressed through

the double-exciton Davydov ansatz:

$$|\mathcal{U}(\mathcal{P}_j\mathcal{U}(\hat{\mu}\Psi_0;t')\otimes|ij\rangle;t)\rangle \equiv$$
$$\sum_{i'j'}^{N} A^{ij}_{i'j'}(t,t')\exp\Big\{\sum_q\big[\lambda^{ij}_{i'j',q}(t,t')\hat{b}^\dagger_q - \text{H.c.}\big]\Big\}\otimes|i'j'\rangle. \quad (50)$$

Here the parameters of the double-exciton ansatz (50) obey the initial (at $t=0$) conditions

$$A^{ij}_{i'j'}(0,t') = \delta_{ii'}\delta_{jj'}A_j(t'), \quad \lambda^{ij}_{i'j',q}(0,t') = \delta_{jj'}\lambda_{j,q}(t'), \quad (51)$$

where $A_j(t')$ and $\lambda_{j,q}(t')$ are determined by the single-exciton ansatz (42). The equations of motion for the parameters $A^{ij}_{i'j'}(t,t')$ and $\lambda^{ij}_{i'j',q}(t,t')$ are given in the Appendix.

Bridging the bra and ket contributions to Eq. (49) yields the explicit expression for the double-exciton response function:

$$\begin{aligned} &G^d(\tau_4,\tau_3,\tau_2,\tau_1) = \\ &\sum_{ijkl}^{N} c_i c_k^*[A_l(\tau_3-\tau_4)]^* A^{ij}_{kl}(\tau_3-\tau_2,\tau_2-\tau_1)\times \\ &e^{-\frac{1}{2}\sum_q\left(|\lambda_{l,q}(\tau_3-\tau_4)|^2+|\lambda^{ij}_{kl,q}(\tau_3-\tau_2,\tau_2-\tau_1)|^2\right)}\times \\ &e^{\sum_q\left([\lambda_{l,q}(\tau_3-\tau_4)]^*\lambda^{ij}_{kl,q}(\tau_3-\tau_2,\tau_2-\tau_1)\right)} + k\leftrightarrow l. \end{aligned} \quad (52)$$

Here $k\leftrightarrow l$ implies the contribution in which the superscripts k and l in A^{ij}_{kl} and $\lambda^{ij}_{kl,q}$ are interchanged.

V. BRIEF SUMMARY OF THE NUMERICAL APPROACH

Let us briefly summarize the obtained results. We have shown that the third-order response is uniquely determined by the four-time correlation function of the transition dipole moments (Eq. (17)) which, in turn, can be represented as a sum of a single-exciton contribution Φ^s (Eq. (27)) and a double-exciton contribution Φ^d (Eq. (28)). In the present work, all high-frequency optically-active vibrational modes are incorporated into the system Hamiltonian, while the bath and the system-bath coupling are responsible for the signal lineshapes. This allows us to represent the single-exciton ($\alpha=s$) and the double-exciton ($\alpha=d$) response functions as a product of system and bath contributions, $\Phi^\alpha = F^\alpha G^\alpha$ (Eq. (33)). The bath contributions F^α are evaluated exactly by the cumulant expansion (Eqs. (36) and (37)). The system response functions are evaluated in terms of the Davydov ansätze. Eqs (46) and (52) deliver the explicit working formulas for G^s and G^d, respectively.

Once the single-exciton and double-exciton four-time correlation functions Φ^s and Φ^d are known, the third-order response functions can be evaluated per Eqs. (22)-(25). According to Eq. (26), they are partitioned into the single- and double-exciton contributions:

$$R_k(t_3,t_2,t_1) = R^s_k(t_3,t_2,t_1) + R^d_k(t_3,t_2,t_1), \quad (53)$$

$k=1,2,3,4$. Here R^s_i involves singly-excited excitonic states only and is responsible for the description of stimulated emission (SE) and ground-state bleach (GSB), while R^d_i is responsible for excited-state absorption (ESA).

Usually, responses must be averaged over orientations of the transition dipole moments $\boldsymbol{\mu}_n$. If reorientation of $\boldsymbol{\mu}_n$ can be neglected on the timescale of the experiment, the (static) orientational averaging can be done analytically as explained in [49]. Inhomogeneous broadening can be taken into account by a series of calculations with different values of the system parameters, e.g. site energies.

Let us discuss computational aspects of the proposed method. Obviously, the evaluation of the bath response functions F^s and F^d presents no difficulties. Computation of the single-exciton response function G^s per Eq. (46) requires the evaluation of two, "forward" and "backward" single-exciton Davydov ansätze. For a N-chromophore molecular aggregate, the evaluation of the single-exciton Davydov ansatz requires integration of $N(N+1)$ (272 in the present case) equations of motion for the parameters A and λ (Eqs. (A6) and (A7)).

Computation of the double-exciton response function G^d per Eq. (52) is much more demanding. Besides the evaluation of two Davydov ansätze mentioned above, we have to evaluate $N(N-1)$ (240 in the present case) double-exciton ansätze (50). The the initial conditions (51) for these ansätze are determined by the solution of the "forward" single-exciton ansatz. The evaluation of each double-exciton ansatz requires integration of $N(N+1)(N-1)/2$ (2042 in the present case) equations of motion for the parameters A and λ (Eqs. (A9) and (A10)).

Obviously, evaluation of $N(N-1)$ double-exciton anstaze is computationally expensive. Fortunately, we need to propagate the double-exciton ansatz during a relatively short time interval of the order of electronic dephasing time. The point is that the time interval $\tau_3-\tau_2$ in the four-time response functions Φ^d corresponds to the time interval t_3 in the response functions R^d_1 and R^d_2 which are necessary for the calculation of the ESA contribution to the photon-echo signal. The system is in its coherence state during t_3. Hence its dynamics is controlled by the electronic dephasing.

VI. ILLUSTRATIVE CALCULATIONS

Femtosecond optical 2D spectra of various J-aggregates have extensively been studied experimentally [61–64] and simulated numerically [61–67]. Several ensemble [68, 69] and single-molecule [70] 2D experiments on double-ring light-harvesting complexes LH2 have been performed. In the present section, we apply the approach of Sections

III and IV for the simulation of electronic 2D spectra of model molecular rings.

A. The model parameters

We consider the so-called toy model of J-aggregates [49], with the tangential (head-to-tail) orientations of the transition dipoles $\hat{\boldsymbol{\mu}}_m$ (see Fig. 1). The site energies are set to zero ($\varepsilon_m = \varepsilon = 0$), and site-independent nearest-neighbor ($J_{m,n} = -J\delta_{m,n\pm1}$) and quadratic ($K_{mn} = K\delta_{m,n\pm1}$) couplings are assumed. We consider both repulsive ($K > 0$) and attractive ($K < 0$) quadratic couplings.

The primary phonon frequency of the B850 ring, ω_0, is in the range of $1000 \sim 1600$ cm^{-1} [59, 60]. In the present work, we set $\omega_0 = 0.124$ eV (~ 1000 cm^{-1}). Hereafter, we employ the dimensionless variables and use ω_0 as the unit of energy. This yields the unit of time of 33.3 fs. The couplings J and K, as well as the phonon bandwidth W and the Huang-Rhys factor S are varied.

We adopt the Drude spectral density of the secondary bath,

$$D(\omega) = 2\eta\omega\frac{\gamma}{\omega^2+\gamma^2}, \tag{54}$$

which yields the lineshape functions [1]

$$\begin{aligned} g(t) \;=\; & \frac{\eta}{\gamma}\coth\frac{\gamma\beta}{2}[e^{-\gamma t}+\gamma t-1] - \\ & i\frac{\eta}{\gamma}[e^{-\gamma t}+\gamma t-1] + \frac{4\eta\gamma}{\beta}\sum_{n=1}^{\infty}\frac{e^{-\nu_n t}+\nu_n t-1}{\nu_n(\nu_n^2-\gamma^2)}. \end{aligned} \tag{55}$$

Here $\nu_n = 2\pi n/\beta$ are the Matsubara frequencies. In our calculations, we set $\eta = 0.05$, $\beta = 5$, and $\gamma = 0.02$.

B. 2D spectra

The so-called rephasing (subscript R) and non-rephasing (subscript NR) contributions to the electronic 2D signals are expressed in terms of the response functions (53) as follows [6–8, 58]:

$$\begin{aligned} R_{\rm R}(t_3,t_2,t_1) \;&= R_2^s(t_3,t_2,t_1) + R_3^s(t_3,t_2,t_1) \\ &\quad -[R_1^d(t_3,t_2,t_1]^* \end{aligned} \tag{56}$$

and

$$\begin{aligned} R_{\rm NR}(t_3,t_2,t_1) \;&= R_1^s(t_3,t_2,t_1) + R_4^s(t_3,t_2,t_1) \\ &\quad -[R_2^d(t_3,t_2,t_1)]^*. \end{aligned} \tag{57}$$

If the laser pulses are short on the time scale of the system dynamics and bath relaxation, the R/NR contributions

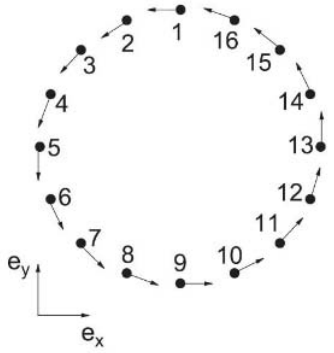

FIG. 1: A sketch of the arrangement of the transition dipole moments of the toy model of the molecular ring with nearest-neighbor inter-chromophore couplings. The unit vectors e_x and e_y label two orthogonal directions in the plane of the ring.

to the 2D signal read

$$\begin{aligned} & S_{\rm R/NR}(\omega_\tau,T_w,\omega_t) \sim \\ & {\rm Im}\int_0^\infty\int_0^\infty dt_3 dt_1 R_{\rm R/NR}(t_3,T_w,t_1)e^{-i\omega_\tau t_3+i\omega_t t_1}. \end{aligned} \tag{58}$$

The total 2D signal is defined by the sum of the two,

$$S(\omega_\tau,T_w,\omega_t) = S_{\rm R}(\omega_\tau,T_w,\omega_t) + S_{\rm NR}(\omega_\tau,T_w,\omega_t). \tag{59}$$

Clearly, both singly- and doubly-excited excitonic states contribute to 2D optical signals of molecular aggregates. Eqs. (27) and (28) reveal that the response functions R_k^s and R_k^d scale with the number of sites as N^2, while any spectroscopic signal should scale as N. Hence the total 2D signal (59) is a result of the partial cancellation of the GSB+SE and ESA contributions.

The cancellations are illustrated by Fig. 2, which shows the GSB+SE contributions (upper panels), the ESA contribution (middle panels), and the total 2D signal $S(\omega_\tau,T_w,\omega_t)$ (lower panels) for different values of the waiting time: $T_w = 0$ (left column), 20 (middle column) and 40 (right column). The nearest-neighbor coupling is moderate, $J = 0.3$, and the quadratic excito-exciton coupling is attractive, $K = -0.2$. The Huang-Rhys factor and the bandwidth are chosen as $S = 0.5$ and $W = 0.8$.

The toy model (for $S = 0$) has a single doubly degenerate optically accessible state with the energy $-2J\cos(\pm\pi) = -0.554$. The spectra of Fig. 2 are computed for a relatively low exciton-phonon coupling ($S = 0.5$) and retain a single-peak structure. At $T_w = 0$, the SE+GSB peak is located at $\omega_\tau = \omega_t \approx -0.89$ (panel (a)). As the waiting time increases, the elongation and the tilt of the peak become less pronounced, and the peak shape tends to be more rounded (compare panels (a), (d), and (g) of Fig. 2).

The ESA contributions are depicted in panels (b), (e), and (h) of Fig. 2. They are negative, as expected. At

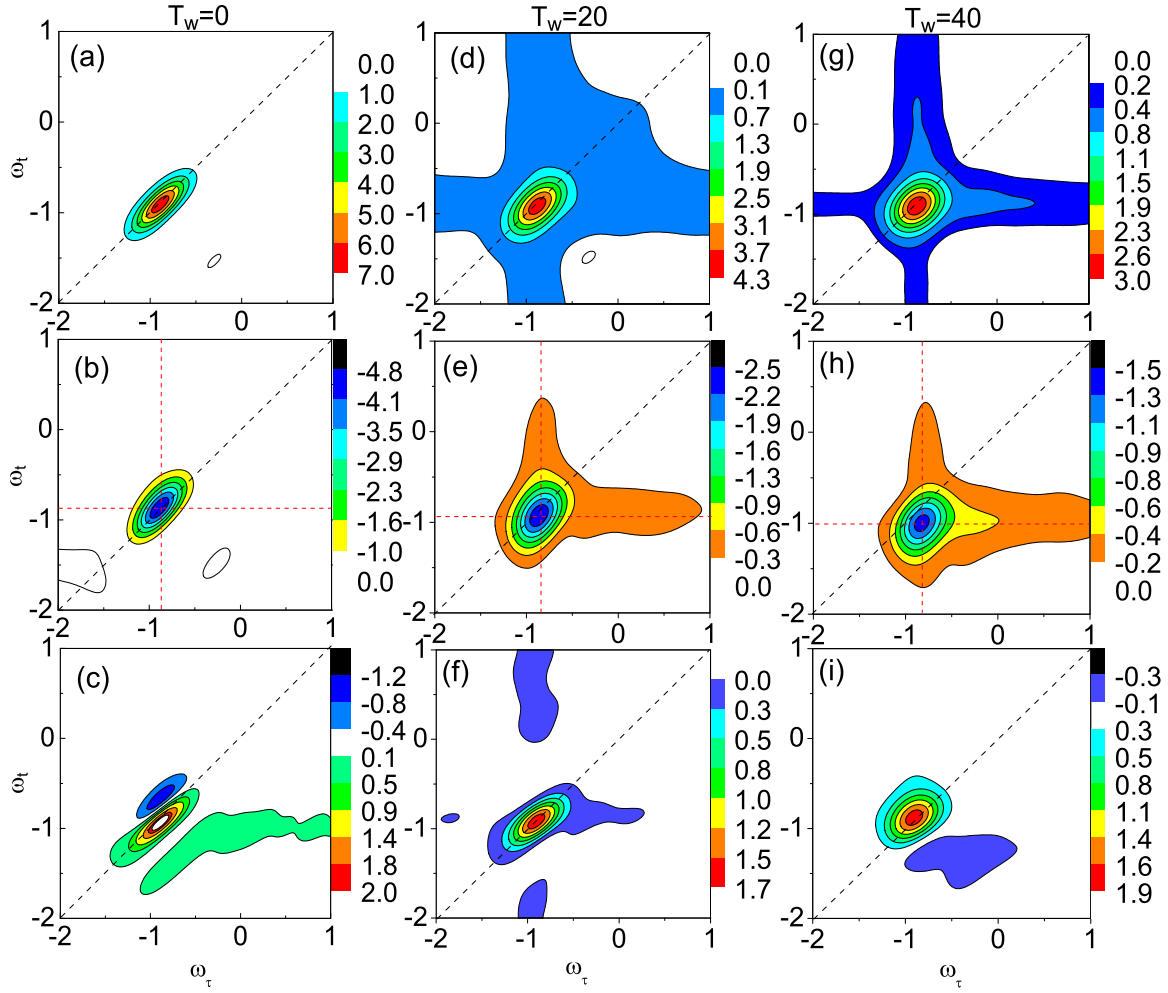

FIG. 2: The GSB+SE contributions (upper panels), the ESA contribution (middle panels), and the total 2D signal $S(\omega_\tau, T_w, \omega_t)$ of the molecular ring (lower panels) for $T_w = 0$ (left column), 20 (middle column) and 40 (right column). The system is characterized by the parameters $J = 0.3$, $K = -0.2$, $S = 0.5$, and $W = 0.8$.

$T_w = 0$, the ESA peak is located at $\omega_\tau = \omega_t \approx -0.88$. As T_w increases, the peak shifts to the red along the ω_t axis (from $\omega_t \approx -0.88$ to $\omega_t \approx -1$), due to the population transfer and energy redistribution in the single-exciton manifold [65]. The T_w evolution of the shape of the ESA peak is similar to that of the GSB+SE peak.

The total 2D signals $S(\omega_\tau, T_w, \omega_t)$ are shown in panels (c), (f), and (i) of Fig. 2. At $T_w = 0$, the signal consists of a positive and negative peaks, which are diagonally elongated. The vertical displacement between the peaks is about 0.28. A weak spectral feature below the main diagonal is a witness of the excitonic coherence. As T_w increases, the two peaks merge, producing a predominantly positive peak. The structure and evolutions of 2D signals discussed above seem to be typical for large J-aggregates [65].

Panel (c) of Fig. 2 should be contrasted with Fig. 3. The latter shows the 2D spectrum at $T_w = 0$, which is calculated for the same molecular ring but with repulsive inter-exciton coupling, $K = 0.2$. Quantitatively, the spectra in panel (c) of Fig. 2 and in Fig. 3 look similar, but certain differences are clearly visible. For example, the shape of the positive peak in Fig. 3 is elliptical, while the shape of its counterpart in panel (c) of Fig. 2 is substantially deformed. On the other hand, the negative lobe of the spectrum in Fig. 3 does not show any simple structure. The shift along the ω_t axis between the positive and negative peaks in Fig. 3 is about 0.26, which is somewhat smaller than that in panel (c) of Fig. 2.

Fig. 4 shows the evolution of 2D spectra in the case of a strong exciton-phonon coupling ($S = 2$) and narrow bandwidth ($W = 0.1$). The spectra exhibit a pronounced vibrational structure (cf. Ref. [49]). Coexistence of positive and negative peaks is a result of the delicate balance

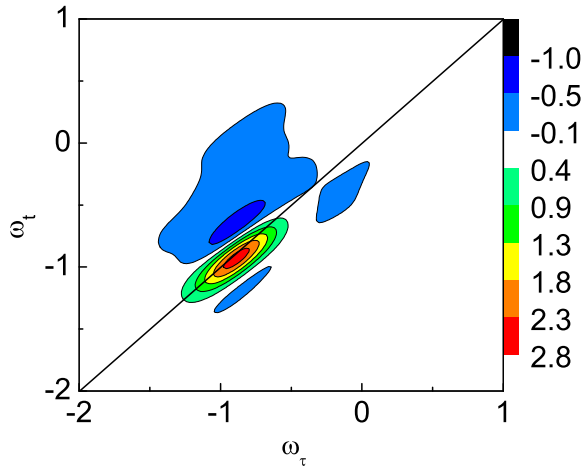

FIG. 3: 2D spectrum $S(\omega_\tau, 0, \omega_t)$ simulated for repulsive exciton-exciton interaction, $K = 0.2$. All other system parameters are the same as for Fig. 2.

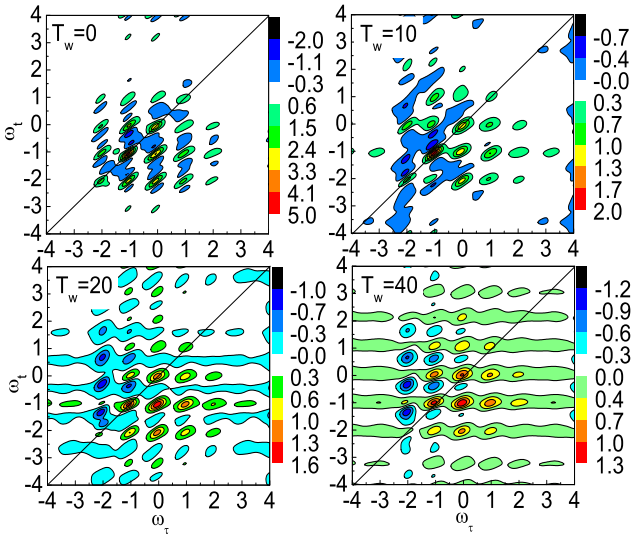

FIG. 4: T_w-evolution of 2D spectra $S(\omega_\tau, T_w, \omega_t)$ simulated for the molecular ring with $J = 0.1$, $K = -0.2$, $S = 2$, and $W = 0.1$. The values of the waiting time T_w are indicated in the panels.

between the GSB and SE on the one hand and the ESA on the other. A slight redshift of the peaks relative their positions at $j\omega_0$, $j = 0, \pm 1, ...$ is due to the inter-exciton coupling (see, e.g., Ref. [52]).

The spectra at $T_w = 0$ and 10 exhibit a number of positive peaks embedded into extended negative spots. As T_w increases, the spectra change their patterns and show progressions of positive and negative peaks. The negative peaks are mostly concentrated above the main diagonal $\omega_\tau = \omega_t$, while the positive peaks are seen, predominantly, below the main diagonal. The T_w-evolution of the peak shapes is qualitatively similar to that shown in Fig. 2. The T_w-evolutions of the intensities of individual peaks exhibit beatings with a characteristic frequency $\sim \omega_0$ (not shown).

VII. CONCLUSION

We have developed a variational approach to the description of four-wave-mixing signals of molecular aggregates, which is based on the evaluation of third-order response functions in terms of the Davydov D_1 ansatz. Our theory treats singly- and doubly-excited excitonic sates, and handles the contributions due to stimulated emission, ground state bleach, and excited state absorption. As an illustration, we have simulated a series of optical 2D spectra for a toy model of J-aggregate.

The present approach does not involve any assumptions on the strength of the exciton-exciton and exciton-phonon coupling. It can straightforwardly be generalized beyond molecular rings towards the description of general molecular aggregates. The effect of inhomogeneous broadening can be accounted for by performing a series of simulations at slightly different system parameters. The present approach is computationally efficient and can potentially be made numerically exact, notably if the exciton dynamics is treated by multi Davydov ansätze (see, e.g., Ref. [71]).

We complete our discussion by noting that in our approach, as outlined in Section IV, the direction of the evolution between the actual times τ_2 and τ_3 is chosen from τ_2 to τ_3. In other words, evolution is considered in the ket-state, which resulted in the expressions, given by Eqs. (45) and (49), respectively. A careful reader have probably noticed that with the same numerical effort the aforementioned evolution can be transferred to the bra-state, resulting in the expressions

$$G^{\rm s}(\tau_4, \tau_3, \tau_2, \tau_1) = \sum_{jk}^{N} c_j c_k^* \langle \mathcal{U}(\mathcal{P}_k \mathcal{U}(\hat{\mu}\Psi_0; \tau_3 - \tau_4); \tau_2 - \tau_3) | \mathcal{P}_j \mathcal{U}(\hat{\mu}\Psi_0; \tau_2 - \tau_1) \rangle. \quad (60)$$

and

$$G^{\rm d}(\tau_4, \tau_3, \tau_2, \tau_1) = \sum_{ijkl}^{N} c_i c_k^* \langle \mathcal{U}(\langle kl| \otimes \langle \mathcal{P}_l \mathcal{U}(\hat{\mu}\Psi_0; \tau_3 - \tau_4)|; \tau_2 - \tau_3)| \times |\mathcal{P}_j \mathcal{U}(\hat{\mu}\Psi_0; \tau_2 - \tau_1)\rangle \otimes |ij\rangle \quad (61)$$

respectively. Naturally, in the case of exact quantum evolution the two sets of expressions would provide identical results. It is easy to show that the above property formally follows from the fact that quantum evolution, being unitary in its nature, preserves the scalar products between the evolving states. Dynamical variational approaches, however, while preserving the norm, do not

necessarily preserve the scalar products. It is easy to show by a direct computation that for the D_1 ansatz in the non-zero exciton sectors the scalar products are not conserved, i.e., $\langle \mathcal{U}(\Psi';t)|\mathcal{U}(\Psi;t)\rangle \neq \langle \Psi'|\Psi\rangle$. On the other hand the D_1 ansatz is exact in the zero-exciton sector, and thus preserves the scalar products. Therefore, the expressions for $G^{\rm s}$ [Eqs. (45) and (60)] provide identical results, whereas their counterparts for $G^{\rm d}$ [Eqs. (49) and (61)] yield different answers. Therefore, the discrepancy of the answers provided by Eqs. (49) and (61) can be viewed as a convenient measure of the performance of the D_1 approach to nonlinear response of molecular aggregates. The quantitative relation between the aforementioned discrepancy and the ansatz error

$$\begin{aligned} \Delta(\Psi) &= \sqrt{\langle d\mathcal{U}(\Psi)+iH\Psi|d\mathcal{U}(\Psi)+iH\Psi\rangle}, \\ d\mathcal{U}(\Psi) &= \left(\frac{d\mathcal{U}(\Psi;t)}{dt}\right)_{t=0} \end{aligned} \tag{62}$$

will be addressed elsewhere.

Acknowledgments

Support from the Singapore National Research Foundation through the Competitive Research Programme (CRP) under Project No. NRF-CRP5-2009-04 is gratefully acknowledged. K.W.S. also thanks NNSF of China (No. 11404084) for partial support. M.F.G. acknowledges support from the Deutsche Forschungsgemeinschaft through the DFG-Cluster of Excellence "Munich-Centre for Advanced Photonics" (www.munich-photonics.de). V.Y.C. acknowledges the support through NSF Grant No. CHE-1111350.

APPENDIX A: DAVYDOV ANSÄTZE FOR SINGLY- AND DOUBLY-EXCITED EXCITONIC STATES

The D_1 ansatz is demonstrated to faithfully reproduce exciton dynamics of molecular rings in a wide range of the exciton-phonon and exciton-exciton couplings [46–48]. In this Appendix, we present the explicit expressions for the evaluation of the D_1 ansätze. To simplify the subsequent notation, we rewrite the explicit formulas for the single- and double-exciton ansätze as follows:

$$\left|\Psi^{s}_{D_1}(t)\right\rangle \approx \sum_m A_m(t)\exp\Big\{\sum_q\left[\lambda_{m,q}(t)\hat{b}^\dagger_q - \text{H.c.}\right]\Big\}\otimes|m\rangle, \tag{A1}$$

$$\begin{aligned} \left|\Psi^{d}_{D_1}(t)\right\rangle \approx& \sum_{m>n} A_{mn}(t)\times \\ & \exp\Big\{\sum_q\left[\lambda_{mn,q}(t)\hat{b}^\dagger_q - \text{H.c.}\right]\Big\}\otimes|mn\rangle. \end{aligned} \tag{A2}$$

Essentially, we have dropped the superscripts and the time moment t' in the parameters A and λ specifying the double-exciton ansatze. The superscripts and t' are explicitly indicated in Eq. (50) to visualize how A and λ depend on the initial conditions (51).

The time evolution of the parameters $A(t)$ and $\lambda(t)$ is generated by the Dirac-Frenkel variational principle [72, 73]. The equations of motion for these parameters,

$$\frac{d}{dt}\left(\frac{\partial L}{\partial \dot{A}^*}\right) - \frac{\partial L}{\partial A^*} = 0. \tag{A3}$$

$$\frac{d}{dt}\left(\frac{\partial L}{\partial \dot{\lambda}^*}\right) - \frac{\partial L}{\partial \lambda^*} = 0, \tag{A4}$$

(all superscripts specifying $A(t)$ and $\lambda(t)$ are dropped here for brevity) are obtained by the variation of the Lagrangian

$$L = \langle \Psi^{\alpha}_{D_1}(t)|\{\frac{i}{2}\left(\frac{\overrightarrow{\partial}}{\partial t} - \frac{\overleftarrow{\partial}}{\partial t}\right) - H_S\}|\Psi^{\alpha}_{D_1}(t)\rangle, \tag{A5}$$

$\alpha = s,\, d$.

A standard derivation yields the equations of motion for the parameters of the single-exciton ansatz (A1) [43–49]:

$$\begin{aligned} -i\dot{A}_m =& \frac{i}{2}A_m\sum_q(\dot{\lambda}_{m,q}\lambda^*_{m,q} - c.c.) - \sum_n J_{mn}A_nS_{m,n} \\ & -\epsilon_m A_m - \sum_q g_q\omega_q A_m(\lambda_{m,q}e^{iqm} + c.c.) \\ & -\sum_q \omega_q A_m|\lambda_{m,q}|^2, \end{aligned} \tag{A6}$$

$$\begin{aligned} iA_m\dot{\lambda}_{m,q} =& \sum_n J_{mn}A_n(\lambda_{n,q}-\lambda_{m,q})S_{m,n} \\ & +g_q\omega_q A_m e^{-iqm} + \omega_q\lambda_{m,q}A_m, \end{aligned} \tag{A7}$$

with the Debye-Waller factor given by

$$S_{m,n} = \exp[-\frac{1}{2}\sum_q(|\lambda_{m,q}|^2 + |\lambda_{n,q}|^2 - 2\lambda^*_{m,q}\lambda_{n,q})]. \tag{A8}$$

A very similar procedure yields the equations of motion for the parameters governing the double-exciton ansatz (A2):

$$\begin{aligned} -i\dot{A}_{mn} =& \frac{i}{2}A_{mn}\sum_q(\dot{\lambda}_{mn,q}\lambda^*_{mn,q} - c.c.) - (\varepsilon_m+\varepsilon_n)A_{mn} \\ & -\sum_q g_q\omega_q A_{mn}(\lambda_{mn,q}e^{iqm} + \lambda_{mn,q}e^{iqn} + c.c.) \\ & -\sum_q \omega_q A_{mn}|\lambda_{mn,q}|^2 - \sum_{n'>m} J_{nn'}A_{mn'}S_{mn,mn'} \\ & -\sum_{n'>n} J_{mn'}A_{nn'}S_{mn,nn'} - \sum_{m'<n} J_{mm'}A_{m'n}S_{mn,m'n} \\ & -\sum_{m'<m} J_{nm'}A_{m'm}S_{mn,m'm} - KA_{mn}\delta_{m,n-1}, \end{aligned} \tag{A9}$$

$$
\begin{aligned}
i\dot{A}_{mn}\dot{\lambda}_{mn,q} &= g_q\omega_q A_{mn}(e^{-iqm}+e^{-iqn}) + \omega_q A_{mn}\lambda_{mn,q} \\
&+ \sum_{n'>m} J_{nn'}A_{mn'}S_{mn,mn'}(\lambda_{mn',q}-\lambda_{mn,q}) \\
&+ \sum_{n'>n} J_{mn'}A_{nn'}S_{mn,nn'}(\lambda_{nn',q}-\lambda_{mn,q}) \\
&+ \sum_{m'<n} J_{mm'}A_{m'n}S_{mn,m'n}(\lambda_{m'n,q}-\lambda_{mn,q}) \\
&+ \sum_{m'<m} J_{nm'}A_{m'm}S_{mn,m'm}(\lambda_{m'm,q}-\lambda_{mn,q}),
\end{aligned}
\tag{A10}
$$

Here

$$
\begin{aligned}
S_{mn,m'n'} &= \exp[-\frac{1}{2}\sum_q(|\lambda_{mn,q}|^2+|\lambda_{m'n',q}|^2 \\
&\quad -2\lambda^*_{mn,q}\lambda_{m'n',q})].
\end{aligned}
\tag{A11}
$$

is the double-exciton Debye-Waller factor.

[1] S. Mukamel, *Principles of Nonlinear Optical Spectroscopy*; Oxford University Press: New York, 1995.
[2] T. Meier, V. Chernyak, and S. Mukamel **107**, 8759 (1997).
[3] Zhang, W. M.; Meier, T.; Chernyak, V.; Mukamel, S. J. Chem. Phys. 1998, 108, 7763.
[4] T. Renger, V. May, O. Kühn. Phys. Rep. **343**,137(2001)
[5] V. I. Novoderezhkin, M. A. Palacios, H. van Amerongen, and R. van Grondelle. J. Phys. Chem. B. **108**, 10363 (2004).
[6] M. Cho, *Two-Dimesional Optical Spectroscopy* (CRC Press, New York, 2009).
[7] S. Mukamel and D. Abramavicius, Chem.Rev. **104**, 2073 (2004).
[8] D. Abramavicius, B. Palmieri, D. V. Voronine, F. Šanda, and S. Mukamel, Chem. Rev. **109**, 2350(2009).
[9] Jansen, T. L. C.; Snijders, J.G.; Duppen, K. *J. Chem. Phys.* **2001**, *114*, 10910-10921.
[10] C. Liand and T. L. C. Jansen, J. Chem. Theory Comput. 8 (2012) 1706.
[11] M. F. Gelin, A. V. Pisliakov, D. Egorova, and W. Domcke, J. Chem. Phys. **118**, 5287 (2003).
[12] R. van Grondelle and V. I. Novoderezhkin, Phys. Chem. Chem. Phys. **8**, 793 (2006).
[13] H. van Amerogen, L. Valkunas, and R. van Grondelle, *Photosynthetic Excitons* (World Scientific, Singapore, 2000).
[14] A. Ishizaki and G. R. Fleming, J. Chem. Phys. **130**, 234110 (2009).
[15] A. Ishizaki and G. R. Fleming, J. Chem. Phys. **130**, 234111 (2009).
[16] Y. Tanimura, J. Phys. Soc. Jpn. **75**, 082001 (2006).
[17] M. H. Beck, A. Jäckle, G. A. Worth, and H. D. Meyer, Phys. Rep. **324**, 1 (2000) .
[18] H. D. Meyer, Comput. Mol. Sci. **2**, 351(2012).
[19] H. Wang and M. Thoss, Chem. Phys. **347**, 139 (2008).
[20] K. H. Hughes, C.D. Christ, and I. Burghardt, J. Chem. Phys. **131**, 024109 (2009).
[21] K. H. Hughes, C.D. Christ, and I. Burghardt, J. Chem. Phys. **131**, 124108 (2009).
[22] J. Prior, A. W. Chin, S. F. Huelga, and M. B. Plenio, Phys. Rev. Lett. **105**, 050404 (2010).
[23] M. P. Woods, R. Groux, A. W. Chin, S. F. Huelga, and M. B. Plenio, J. Math. Phys 55, 032101 (2014).
[24] N. Makri and D. E. Makarov, J. Chem. Phys. 102, 4600 (1995).
[25] N. Makri and D. E. Makarov, J. Chem. Phys. 102, 4611 (1995).
[26] R. Doll, D. Zueco, M. Wubs, S. Kohler, and P. Hänggi, Chem. Phys. **347**, 243 (2008).
[27] M. F. Gelin, D. Egorova, and W. Domcke, Phys. Rev. E **84**, 041139 (2011).
[28] P. Nalbach, D. Braun, and M. Thorwart, Phys. Rev. E 84, 041926 (2011).
[29] D. M. Wilkins and N. S. Dattani, arXiv:1411.3654v2.
[30] B. Hein, C. Kreisbeck, T. Kramer, and M. Rodriguez, New J. Phys. 14, 023018 (2012).
[31] L. Chen, R. Zheng, Y. Jing, and Q. Shi, J. Chem. Phys. 134, 194508 (2011).
[32] Shu-Hao Yeh and S. Kais, J. Chem. Phys. 141, 234105 (2014).
[33] Y. Tanimura, J. Chem. Phys. 137, 22A550 (2012).
[34] M. F. Gelin, D. Egorova, and W. Domcke, Acc. Chem. Res. 42 (2009) 1290.
[35] M. F. Gelin, D. Egorova, and W. Domcke, J. Chem. Phys. 131 (2009) 194103.
[36] J. Krčmář, M. F. Gelin, and W. Domcke, Chem. Phys. 422, 53 (2013).
[37] A. S. Davydov and N. I. Kislukha, Phys. Status Solidi B **59**, 465 (1973).
[38] A. S. Davydov, *Solitons in Molecular Systems* (Reidel, Dordrecht, 1985).
[39] M. J. Šrinjar, D. V. Kapor, and S. D. Stojanović, Phys. Rev. A. **38**, 6402 (1988).
[40] L. Cruzeiro-Hansson, Phys. Rev. Lett. **73**, 2927 (1994).
[41] Y. Yao and Y. Zhao, J. Chem. Phys. **139**, 014102 (2013).
[42] N. Wu, L.W. Duna, X. Li and Y. Zhao, J. Chem. Phys. **138**, 084111 (2013).
[43] J. Sun, B. Luo, and Y. Zhao, Phys. Rev. B. **82**, 014305 (2010).
[44] B. Luo, J. Ye, C. B. Guan, and Y. Zhao, Phys. Chem. Chem. Phys. **12**, 15073 (2010).
[45] B. Luo, J. Ye, Y. Zhao, Phys. Status Solidi C **8**, 70 (2011).
[46] G.C. Yang, N. Wu, T. Chen, K.W. Sun, and Y. Zhao, J. Phys. Chem. C **116**, 3747 (2012).
[47] J. Ye, K. W. Sun, Y. Zhao, Y. J. Yu, C. K. Lee, and J. S. Cao, J. Chem. Phys. **136**, 245104 (2012).
[48] K. W. Sun, J. Ye, and Y. Zhao, J. Chem. Phys. **141**, 124103 (2014).
[49] T. D. Huynh, K. W. Sun, M. Gelin, and Y. Zhao, J. Chem. Phys. **139**, 104103 (2013).

[50] V. Chernyak and S. Mukamel, J. Chem. Phys. **105**, 4565 (1996).

[51] G. D. Mahan, *Many Particle Physics*, 3rd ed. (Springer, Dordrecht, 2000).

[52] L. Chen, M. F. Gelin, W. Domcke, and Y. Zhao, J. Chem. Phys. **142**, 164106 (2015).

[53] S. Tanaka, J. Chem. Phys. **119**, 4892 (2003).

[54] The quotation marks reflect the fact that, as noted earlier, the actual times τ_k are not necessarily chronologically ordered within our approach.

[55] L. Cruzeiro-Hansson, Phys. Rev. E 66, 023901 (2002).

[56] D. Kapor, M. Skrinjar, Z. Ivic, and Z. Przulj, Phys. Rev. E 73, 013901 (2006).

[57] Note that two-exciton state defined per Eq. (47) can be considered as a multi Davydov ansatz of multiplicity 2, where each exciton state is specified by two amplitudes and two sets of coherent states. Hence the problem of propagation of $N(N-1)$ double-exciton Davydov ansätze can be reduced to the propagation of a single double-exciton ansatz of multiplicity 2. Work in this direction is currently in progress.

[58] R. Venkatramani and S. Mukamel, J. Chem. Phys., **117**, 11089 (2002).

[59] A. Damjanović, I. Kosztin, U. Kleinekathöfer, and K. Schulten, Phys. Rev. E **65**, 031919 (2002).

[60] L. Janosi, I. Kosztin, and A. Damjanović, J. Chem. Phys. **125**, 014903 (2006).

[61] I. Stiopkin, T. Brixner, M. Yang, and G. R. Fleming, J. Phys. Chem. B **110**, 20032(2006).

[62] J. M. Womick, S. A. Miller, and A. M. Moran, J. Phys. Chem. A **113**, 6587 (2009).

[63] J. M. Womick, S. A. Miller, and A. M. Moran, J. Phys. Chem. B **113**, 6630 (2009).

[64] F. Milota, V. I. Prokhorenko, T. Mancal, H. von Berlepsch, O. Bixner, H. F. Kauffmann, and J. Hauer, J. Phys. Chem. A, 117, 6007 (2013).

[65] V. Butkus, A. Gelzinis, and L. Valkunas, J. Phys. Chem. A **115**, 3876(2011).

[66] A. G. Dijkstra, T. la C. Jansen, and J. Knoester, J. Chem. Phys. **128**, 164511(2008).

[67] J. Han, H. Zhang, and D. Abramavicius, J. Chem. Phys. **139**, 034313 (2013).

[68] E. E. Ostroumov, R. M. Mulvaney, J. M. Anna, R. J. Cogdell, and G. D. Scholes, J. Phys. Chem. B 117, 11349 (2013).

[69] E. Harel and G. S. Engel, Proc. Natl. Acad. Sci. USA **109**, 706 (2012).

[70] S. Tubasum, R. Camacho, M. Meyer, D. Yadav, R. J. Cogdell, T. Pullerits, and I. G. Scheblykin, Phys. Chem. Chem. Phys. 15, 19862 (2013).

[71] N. Zhou, L. Chen, Y. Zhao, D. Mozyrsky, V. Chernyak,and Y. Zhao, Phys. Rev. B 90, 155135 (2014).

[72] P. A. M. Dirac, Proc. Cambridge Philos. Soc. **26**, 376 (1930).

[73] J. Frenkel, *Wave Mechanics* (Oxford University Press, New York, 1934).